

Dynamic Coefficient β Curve Determination

Song Jun Hwang*¹, Jong Hyok Kim and Song Hyok Mun¹, Myong Il Rim¹

¹ Faculty of Civil Engineering Pyongyang University of Architecture, D P R Korea

*Corresponding Author: dawei_0110@163.com

ARTICLE INFO

Article history:

Received 24-4-2024

Revised 7-8-2024

Accepted 14-8-2024

Available online 31-8-2024

E-ISSN: 2622-1640

P-ISSN: 2622-0008

How to cite:

Hwang, S. J. et al. Dynamic Coefficient β Curve Determination. International Journal of Architecture and Urbanism. 2024. 8(2):291-316.

ABSTRACT

This study presents a comprehensive methodology for determining the parameters of the dynamic coefficient β curve, which is crucial in assessing the magnitude of seismic actions on structures. We propose a novel approach to identify the excellent period of seismic waves and establish the design values for the dynamic coefficient curve. Our analysis focuses on the descent interval, branch points, and the acceleration response spectrum, particularly for cases where $T=10$ seconds. By integrating statistical analysis with seismic response characteristics, we refine the β - T curve to enhance its applicability in aseismic design standards. Our findings demonstrate that the proposed β curve model aligns closely with empirical seismic data, offering improved safety and reliability for structures with extended natural vibration periods. This research contributes to advancing the understanding and implementation of seismic design principles, ensuring better structural resilience against earthquakes.

Keywords: dynamic coefficient; β curve; structure; acceleration



This work is licensed under a Creative Commons Attribution-ShareAlike 4.0 International.
<http://doi.org/10.32734/ijau.v8i2.16243>

1. Introduction

The response spectral theory, introduced by Biot in 1934, has become a cornerstone in seismic analysis and structural engineering. This theory provides a framework for determining the magnitude of seismic actions and analyzing the seismic response of structures. Biot's approach considers the distribution of mass and the vibration modes of buildings, which vary with height, to accurately assess seismic impacts. In seismic design, the dynamic coefficient β curve plays a critical role in quantifying the seismic forces that structures must withstand [1] [2] [3]. This curve is integral to the development of aseismic design standards, as it reflects the relationship between the maximum absolute acceleration response and the ground acceleration in a single-degree-of-freedom system. The β curve is influenced by various factors, including the natural vibration period of the structure and the geographic characteristics of the site. Despite its importance, the determination of the dynamic coefficient β curve requires careful consideration of several parameters, such as the excellent period of seismic waves, the design value of the dynamic coefficient, and the acceleration response spectrum [4] [5] [6]. This study aims to refine the β curve model by integrating statistical analysis with empirical seismic data, thereby enhancing its applicability in modern aseismic design standards. Our research focuses on the descent interval, branch points, and the acceleration response spectrum, particularly for cases where the natural vibration period T equals 10 seconds. By improving the β curve's accuracy and reliability, we contribute to

advancing seismic design practices and ensuring the structural resilience of buildings in earthquake-prone areas [7] [8] [9].

$$F_{ji} = K_E \cdot \beta_j \cdot \eta_{ji} \cdot G_i \tag{1}$$

F_{ji} - seismic action at the i th point in the j -difference vibration shape

K_E - seismic activity control coefficient

β_j -Dynamic coefficients along the j th vibration

η_{ji} - vibration shape coefficients at the i th mass in the j -difference vibration shape

G_i - i th mass's weight

In the equation 1, β is taken on the dynamic coefficient β curve.

K_E is a factor that guarantees the strength of an earthquake that can be encountered on the site, which depends on the geographic features of the area and is specified differently from country to country.

The vibration shape coefficient η_{ji} is calculated as follows:

$$\eta_{ji} = X_{ji} \sum_{i=1}^n X_{ji} G_i / \sum_{i=1}^n X_{ji}^2 G_i \tag{2}$$

X_{ji} -the relative horizontal displacement of the i th mass in the j th natural vibration shape

Thus, η_{ji} is unintentionally determined according to the dynamic properties of the structure.

β obtains a statistical value of the ratio of the maximum absolute acceleration response and ground acceleration of the single-degree-of-freedom system, which is defined and written differently from country to country.

The dynamical coefficient β curve reflected in the aseismic design standard of our country is the same as Fig 1. Here the maximum value of the acceleration response spectrum $\beta_{max}=2.3$. ([1])

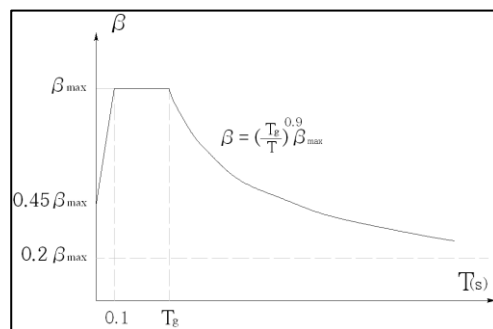


Figure 1 the β curve reflected in aseismic design standard

In Fig. 1, T_g is the excellent period of the base, T is the natural vibration period of the structure.

The Aseismic Design Standards (GB 5011-2010) of the People's Republic of China uses the seismic influence coefficient curve multiplied by the seismic action adjustment factor K_E to the acceleration response spectral value β , as Equation 3 (GB 5011-2010), which is essentially the same as the accelerometer response spectral curve in nature because K_E is a constant value according to the type of construction site. [2].

$$\alpha = K_E \cdot \beta \tag{3}$$

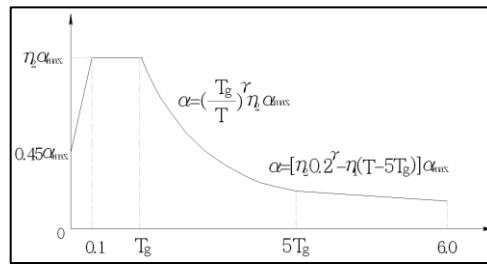


Figure 2 The seismic influence coefficient α curve of the Chinese aseismic design standard

The damping index γ of the curve descent step is as follows:

$$\gamma = 0.9 + \frac{0.05 - \zeta}{0.3 + 6\zeta} \tag{4}$$

The slope adjustment coefficient η_1 of the straight-down step is determined as the following.

$$\eta_1 = 0.02 + \frac{0.05 - \zeta}{4 + 32\zeta} \tag{5}$$

The attenuation coefficient η_2 is defined as the following.

$$\eta_2 = 1 + \frac{0.05 - \zeta}{0.08 + 1.6\zeta} \tag{6}$$

In GB 5011-2010, β_{max} is 2.25. [2]

In Fig. 2, T_g is the excellent period of the base, T is the natural vibration period of the structure.

As the dynamic coefficient β curve of ASCE 7 is shown in Fig 3, the β curve in the long period interval, $T > T_L$, descends to the exponential form of $1/T^2$. (The maximum is divided into five groups of 4, 6, 8, 12, and 16 s according to the site category) [2].

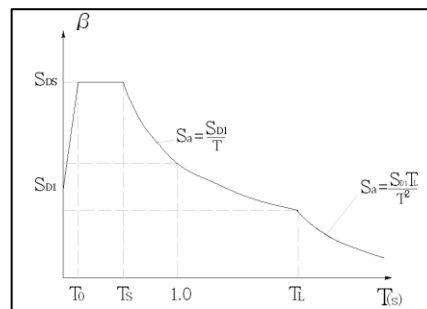


Figure 3 The β curve of ASCE 7

2. Method

This study involves collecting seismic data from various sources, including historical earthquake records and accelerometer data. Fourier transform analysis is employed to determine the excellent period of seismic waves, identifying the period at which the power spectrum peaks. The dynamic coefficient β curve is analyzed by initially estimating parameters through statistical analysis of the maximum absolute acceleration response and ground acceleration. The model is refined by fitting empirical data to a theoretical curve, validated against existing seismic standards. Statistical analysis assesses the distribution of β_{max} values, and sensitivity analysis validates the model by examining the effects of varying natural vibration periods and damping ratios. This methodology provides a

rigorous framework for determining the dynamic coefficient β curve, enhancing its applicability in modern seismic design standards.

3. Result and Discussion

The seismic response and acceleration response spectra of single-degree-of-freedom systems

To enhance and expand the theoretical discussion related to the provided sentences, consider the following revision: The seismic response of a single-degree-of-freedom (SDOF) system is a foundational aspect of aseismic design and analysis. This is because the SDOF system's seismic response serves as a fundamental model for understanding the behavior of more complex structural systems during seismic events [10] [11] [12]. The dynamic coefficient curve, which corresponds to the acceleration response spectrum of the SDOF system, is crucial in quantifying the magnitude of seismic actions in response spectral analysis. This curve provides insights into the maximum expected ground acceleration and helps in designing structures that can withstand seismic forces effectively. By accurately determining the parameters of the dynamic coefficient β curve, including the excellent period of seismic waves and the descent interval, engineers can enhance the reliability and safety of buildings. This study advances the understanding of the β curve by integrating empirical seismic data with theoretical modeling, ensuring its applicability in modern seismic design standards and contributing to the development of resilient infrastructure.

When an earthquake is encountered in a free diagram such as a in Fig. 4, it oscillates like the b of Fig. 4.

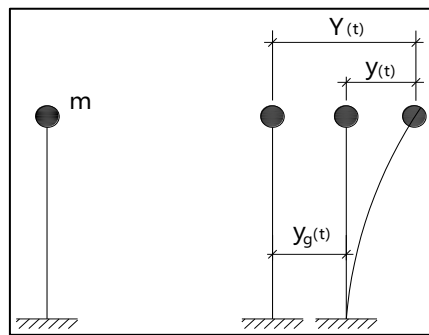


Figure 4 The vibration of a single-degree system

Then the absolute displacement $Y(t)$ of the mass m , consists of a rigid-body displacement $y_g(t)$ along the basis and of a displacement $y(t)$ of the mass m , i.e., the sum of the relative displacement to the base, which occurs when the structure is elastic.

Let's establish the vibration equation of the system.

The working forces of the system are resilience $ky(t)$, resistivity $c\dot{y}(t)$ and inertia forces $m[\ddot{y}_g(t) + \ddot{y}(t)]$, and these are balanced.

Establishing the equilibrium equation is as follows.

$$-m[\ddot{y}_g(t) + \ddot{y}(t)] - ky(t) - c\dot{y}(t) = 0 \quad (7)$$

or
$$m\ddot{y}(t) + ky(t) + c\dot{y}(t) = -m\ddot{y}_g(t) \quad (8)$$

$$\omega^2 = \frac{k}{m}, \quad \zeta = \frac{c}{2\sqrt{km}} = \frac{c}{2\omega m} \quad (9)$$

Eq 1 is the following:.

$$\ddot{y}(t) + 2\zeta\omega\dot{y}(t) + \omega^2 y(t) = -\ddot{y}_g(t) \quad (10)$$

The general solution of Eq. (10) consists of the general solution of the corresponding homogeneous equation and the sum of the specific solutions of the non-homogeneous equation and becomes as follows.

$$y(t) = e^{-\zeta\omega t} \left[y(0) \cos \omega' t + \frac{\dot{y}(0) + \zeta\omega y(0)}{\omega'} \sin \omega' t \right] - \frac{1}{\omega'} \int_0^t \ddot{y}_g(\tau) e^{-\zeta\omega(t-\tau)} \sin \omega'(t-\tau) d\tau \tag{11}$$

In Eq. (11), ω' is the eigen frequency of the one-degree-of-freedom system with attenuation and has the following relation to the eigen frequency ω without attenuation.

$$\omega' = \sqrt{1 - \zeta^2} \omega \tag{12}$$

The damping ratio of the concrete material is 0.05, which is $\omega' = 0.9987 \omega \approx \omega$.

Also $y(0)$ and \dot{y} are the initial displacement and initial velocity at $t=0$.

In general, the initial displacement and initial velocity of the building before an earthquake occur are considered to be 0, so in Eq. (11), the first term becomes 0, and the displacement response of the one-degree system is represented by the afterward harbour.

The derivative $\dot{y}(t)$ of $y(t)$ is the velocity response to the ground and can be written as follows:

$$\dot{y}(t) = \frac{dy(t)}{dt} = - \int_0^t \ddot{y}_g(\tau) e^{-\zeta\omega(t-\tau)} \cos \omega'(t-\tau) d\tau + \frac{\zeta\omega}{\omega'} \int_0^t \ddot{y}_g(\tau) e^{-\zeta\omega(t-\tau)} \sin \omega'(t-\tau) d\tau \tag{13}$$

Substituting Equation (12) and (13) to Equation (10), the absolute acceleration of the system can be found as follows.

$$\begin{aligned} \ddot{y}(t) + \ddot{y}_g(t) &= -2\zeta\omega\dot{y}(t) - \omega^2 y(t) = \\ &= 2\zeta\omega \int_0^t \ddot{y}_g(\tau) e^{-\zeta\omega(t-\tau)} \cos \omega'(t-\tau) d\tau - \\ &\quad - \frac{2\zeta^2\omega^2}{\omega'} \int_0^t \ddot{y}_g(\tau) e^{-\zeta\omega(t-\tau)} \sin \omega'(t-\tau) d\tau + \\ &\quad + \frac{\omega^2}{\omega'} \int_0^t \ddot{y}_g(\tau) e^{-\zeta\omega(t-\tau)} \sin(t-\tau) d\tau \end{aligned} \tag{14}$$

The seismic response is obtained by Equation (11), (13), (14).

However, the recording $\ddot{y}_g(t)$ of the ground acceleration is a random process and cannot be expressed as a function, so the seismic response can be obtained only by numerical integration.

Now let us simply try Equation (14) with

$$S_a = \left| \ddot{y}(t) + \ddot{y}_g(t) \right|_{\max} \tag{15}$$

Here.

Sa-The maximum absolute acceleration response of the SDOF system

① The damping ratio ζ is very small (0.05 for concrete material, 0.02 for steel material), neglecting the ζ and τ^2 terms in the expressions.

②. $\omega' = \omega$

$\sin(t-\tau)$ and $\cos(t-\tau)$ have the same maximum value as the phase difference is $\pi/2$.

Then, S

$$S_a = \left| \ddot{y}(t) + \ddot{y}_g(t) \right|_{\max} = \omega \int_0^t \ddot{y}_g(\tau) e^{-\zeta\omega(t-\tau)} \sin \omega(t-\tau) d\tau \quad (16)$$

The inertia force in a free-conductor system is then influenced by an earthquake on the structure, and the magnitude of the seismic action is as follows.

$$F = |F(t)|_{\max} = mS_a = m \left| \ddot{y}(t) + \ddot{y}_g(t) \right|_{\max} = mg \frac{S_a}{|\ddot{y}_g(t)|} \cdot \frac{|\ddot{y}_g(t)|}{g} = K_E \cdot \beta \cdot G \quad (17)$$

$G = mg$: mass weight

$$\beta = \frac{S_a}{|\ddot{y}_g(t)|_{\max}} \quad (18)$$

β – Dynamic coefficient

K_E – seismic activity control coefficient

$$K_E = \frac{|\ddot{y}_g(t)|_{\max}}{g} \quad (19)$$

Now if $\omega = 2\pi/T$ is placed in Equation (18), then the following is:

$$\beta = \frac{S_a}{|\ddot{y}_g(t)|_{\max}} = \frac{2\pi}{T} \cdot \frac{1}{|\ddot{y}_g(t)|_{\max}} \left| \int_0^t \ddot{y}_g(\tau) e^{-\zeta \frac{2\pi}{T}(t-\tau)} \sin \frac{2\pi}{T}(t-\tau) d\tau \right|_{\max} \quad (20)$$

β is the maximum absolute acceleration response, calculated as S_a , and given the damping ratio ζ of the ground acceleration recording and structural material, we can calculate the dynamical coefficient β for different natural vibration periods T by Eq. (20).

The shape of the β - T curve is in perfect agreement with the acceleration response spectral curve, but the only other point is that the longitudinal coordinate value is dimensionless.

The determination of β_{\max}

In the β - T curve, β_{\max} finds the mean value in the interval with the maximum value of the acceleration response spectral curve based on the concrete material ($\zeta=0.05$).[3]

$$\beta_{\max} = \bar{\beta}(T) = \frac{\sum_{i=1}^n \beta_i(T) |_{\zeta=0.05}}{n} \quad (21)$$

From Fig. 1 to 3, it can be seen that β increases sharply from $T=0$ s to some small period (0.1 s in Fig, 1, 2) and then reaches the max, and again decreases sharply from the point of its excellent period.

Value determination of β when $T=0$ s

If we look at Eq. 20, we can't get it because β is infinite when $T=0$ s.

Therefore, in the actual calculation, the calculated value of β is calculated at a very small value of about $T=0.05$ s.

So what is the β when $T = 0$ s strictly?

$T = 0$ s means that the structure becomes rigid and does not oscillate at all.

In this case, the acceleration response by the ground acceleration does not extend.

Because the structure does not oscillate at all, the input acceleration value is the output acceleration value.

That is, $\beta = 1.0$.

Determination of the minimum value of the natural vibration period of the structure reaching β_{max}

The determination of the dynamic coefficient β curve is crucial in understanding seismic responses. It has been previously confirmed that β equals 1.0 when the natural vibration period $T = 0$ seconds [13] [14]. Although some β - T curves inaccurately equate β at $T = 0$ with β_{max} , it is essential to recognize that the acceleration response typically reaches β_{max} when T is relatively small. Initially, β is assumed to have a value of β_{max} and remains constant until the excellent period T_g , after which it descends following a hyperbolic function. However, most countries' aseismic design standards specify a minimum natural vibration period T at which β reaches β_{max} , as illustrated in Figures 1-3. It is important to note that β is a random variable in the β - T curve, leading to significant variability. This study's statistical analysis reveals that the mean and standard deviation of the minimum T value at the first peak point, where β increases and then sharply declines, are 0.1127 and 0.0351, respectively. This analysis supports the scientific determination of a minimum T value of 0.1 seconds for the β - T curve, ensuring safety in seismic action magnitude assessments.

In the present study, the statistical analysis of the value of T of the first peak point, where β grows continuously and declines sharply, shows that the mathematical means and standard deviations of the minimum value of T are 0.1127 and 0.0351.

Drawing a column diagram for estimating the probability density function from 0.04 to 0.51 with a class size of 0.02 is the same as Fig. 5.

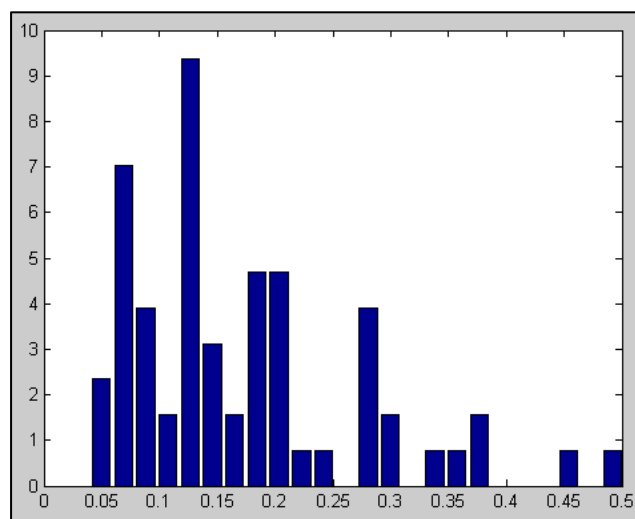


Figure 5 Minimum column diagram of the natural vibration period of the structure reaching β_{max}

The figure shows that in the very β -T curve, β is highly irregular, with very difficulty in defining the minimum distribution of a rapidly rising T.

According to the values of Fig. 5 and the calculated results, it can be seen that it is scientific to see the minimum value of T in the β -T curve to be 0.1 s, and that it gives a safe value even in the determination of the magnitude of seismic action.

Thus, in this study, we propose to use 0.1 s as in the present reference book 1.

Excellent period determination of seismic waves

In the study of seismic wave characteristics, the frequency characteristic, often referred to as the excellent period, is a crucial parameter. This period represents the point at which the power spectrum of the seismic wave reaches its peak, providing essential insights into the wave's potential impact on structures [15] [16] [17]. Accurately determining the excellent period is vital for effective seismic analysis and design. When selecting seismic waves for time history analysis, it is important to choose waves with an excellent period that closely matches the natural vibration period of the construction site. This alignment ensures that the seismic analysis accurately reflects the site's conditions, leading to more reliable and effective aseismic design. Methods such as Fourier transform analysis are employed to precisely identify the excellent period, enhancing the accuracy of seismic response predictions. By integrating empirical data with theoretical models, this study contributes to the development of a scientifically robust dynamic coefficient β curve, ensuring its applicability in modern seismic design standards and improving the safety and resilience of structures subjected to seismic forces.

The excellent period of the seismic wave usually converts the acceleration time history data of seismic waves into Fourier transform to determine the period of the point at which the power is greatest as in Fig. 6.

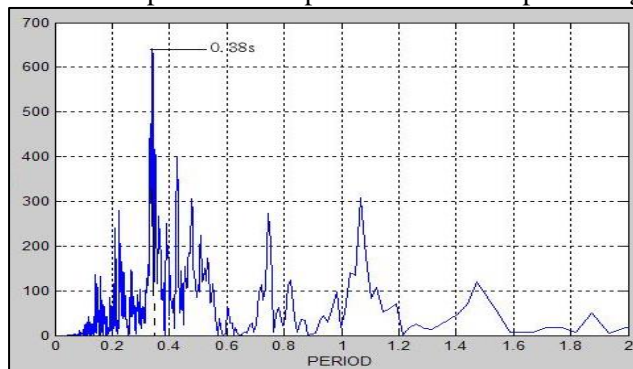


Figure 6 excellent period determination of seismic waves by Fourier transform

In the case of a similar peak, such as Fig. 7, it is impossible to distinguish which is the true excellent period.

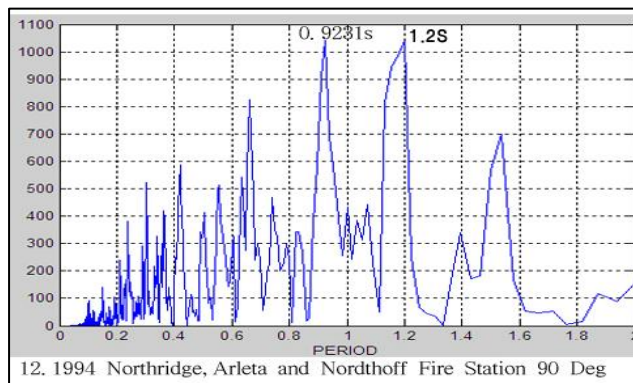


Figure 7 The output spectrum of the 1994 Northridge, Arleta and Nordthoff Fire Station 90 Deg

This shows that the problem of determining the order of excellent period of seismic waves should not be studied only by means of the "signal processing theory" or "seismic engineering" method of dealing with ordinary

time series data, but in conjunction with the "aseismic engineering" method of studying the seismic response characteristics of the structure.

The Fourier transform $X(T)$ of the time series $x(t)$ is as follows:

$$X(T) = \int_{-\infty}^{\infty} x(t)e^{\frac{-i2\pi}{T} t} dt \quad (22)$$

In comparison with Equations (21) and (22), the difference is essentially the same and the difference is that Equation (21) contains the damping ratio ζ of the material.

In the dynamical coefficient β - T curve, the acceleration response decreases sharply at the point of excellent period.

Thus, when $\zeta=0$, it can be speculated that the point of sharp descent in the β - T curve acceleration response spectral curve and the point of excellent period of the seismic wave obtained with the Fourier transform coincide.

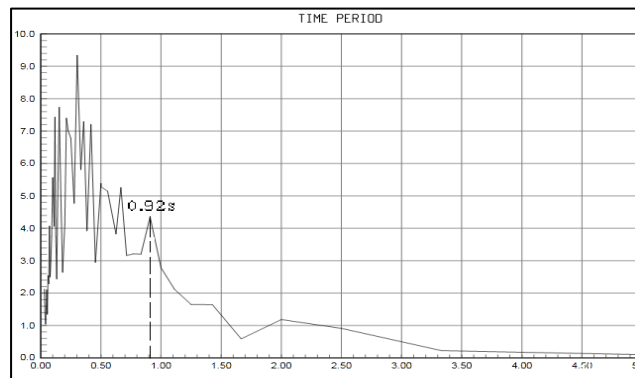


Figure 8 Acceleration response spectrum of 1994 Northridge, Arleta and Nordthoff Fire Station 90 Deg (damping ratio $\zeta=0$)

In Fig. 8, it is clear that the excellent period of the seismic wave is 0.92 s.

In this way, the excellent period of the seismic wave is determined and presented in Appendix 1.

The determination of β_{max}

In the present study, with the results of the calculation of the damping ratio $\zeta = 0.05$ of concrete material based on the dynamical coefficient curve, β from the smallest period in which the acceleration response in the accelerometer response spectral curve was sharply increased to a period of 0.05 s to a period of sharply smaller magnitude, yielding and controlling the calculated results of 7958 points according to 72 seismic waves presented in the appendix.

The mean value of the sample $m = 2.215$ the standard deviation $S = 0.4692$.

Fig. 9 is a column diagram for estimating the probability density function of β_{max} when the magnitude of the class is 0.2, and a probability density function graph of the Gaussian normal distribution with mathematical mean values and standard deviation of 2.215 and 0.469.

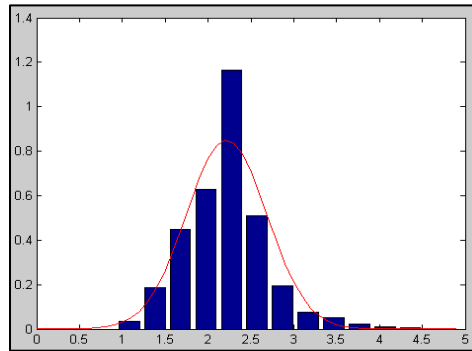


Figure 9 Column diagram and probability density function curve of β_{max}

Fig. 9 shows that the distribution of β_{max} is very close to the normal distribution.

To confirm that the distribution of β_{max} is a normal distribution, a statistical hypothesis test was performed, which did not obtain the basis for acceptance as a normal distribution.

Using the normplot function of Matlab that visually shows the fitness of the normal distribution, the plot is shown as Fig. 10.

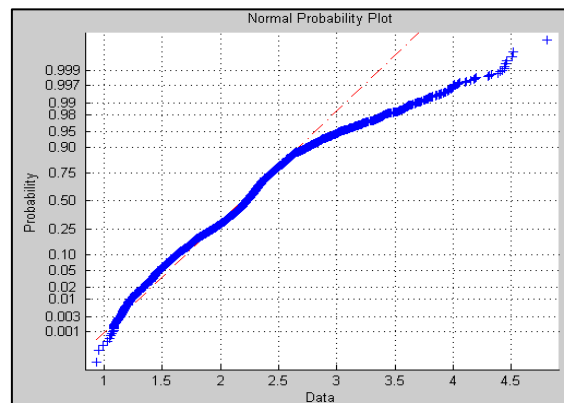


Figure 10 Fitness verification of the normal distribution for the sample sequence by normplot

Figure 10 shows that the distribution of β_{max} from 1.1 to 2.65, where the mean value of 2.215 belongs, depends on the normal distribution. However, since the value of β_{max} is above 2.65, it is shown that the sample values are rapidly departing from the normal distribution.

However, as is typically the case in experimental planning methods, it is not feasible to eliminate abnormalities using a deception test because β_{max} values are derived from actual seismic records. Consequently, it is unreasonable to attempt this through an angle test or by forcing the sample sequence into a normal distribution, as the actual calculation results and the statistical characteristics of the newly configured sample sequence differ from the original ones. This discrepancy arises because seismic acceleration recording is a highly irregular and abnormal random process that defies conventional pattern recognition. Therefore, we assert that a convincing β_{max} does not conform to a normal distribution across the entire computational value interval. However, near the mean of β_{max} , it is reasonable to estimate its confidence limit value.

x_1, x_2, \dots, x_n is generally referred to as sample random variables of size n , and if n is large enough when we do not know the population squared deviation, the confidence interval of the population mean m with confidence probability p is as follows.

$$\left(m - x_p \cdot \frac{S}{\sqrt{n-1}}, m + x_p \cdot \frac{S}{\sqrt{n-1}} \right) \quad (23)$$

$$\frac{1}{\sqrt{2\pi}} \int_0^{x_p} e^{-\frac{z^2}{2}} dz = \frac{p}{2}$$

Here, x_p is the value of

$$x_{0.05}=2.0$$

Estimating the confidence interval of β_{max} with a 95% confidence rate is as follows.

$$\begin{aligned} \beta_{max} &= (2.215 - 2.0 \cdot \frac{0.469}{\sqrt{7957}}, 2.215 + 2.0 \cdot \frac{0.469}{\sqrt{7957}}) = \\ &= (2.205 \sim 2.225) \end{aligned}$$

Thus, $\beta_{max}=2.2$

Decision of the descent interval of β_{max}

As the lower limit value in Reference 1 is $(T_g/T) 0.9\beta_{max}=0.2\beta_{max}$, Fig. 1 equals Fig. 11.

That is, the dynamical coefficient curve from $6T_g$ becomes the horizontal line again.

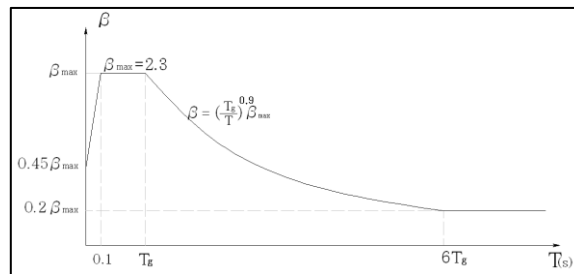


Figure 11 The dynamical coefficient β curve redrawn Fig. 1

On the other hand, in almost every country's aseismic design standard, for example, if it descends into (T_g/T) fractional function as in Fig. 3, the dynamical coefficient curve becomes a horizontal line again at $5T_g$.

This is, after all, that the bifurcation point of the $1/T$ descent region of the dynamical coefficient beta curve is at $5T_g$ to $6T_g$.

In the present study, considering the results, the acceleration response spectral curve descends to a $1/T$ function up to its median $5.5 T_g$. However, as shown in Appendix 1, the curve continues to descend as the natural vibration period of the structure increases. Therefore, in Figures 2 and 3, unlike Figure 1, there is no horizontal interval in the acceleration response spectral curve. The dynamic coefficient curve descends in two ways: first, it descends to the hyperbolic form of a fractional function, as seen in UBC 97, where a relatively long natural oscillation period results in an excessively small acceleration response, weakening structural safety. Second, the descending section is divided into two parts, initially descending to a $1/T$ function and then transitioning to a $1/T^2$ function at a branch point or to a slope, as depicted in Figures 2 and 3. This approach is scientific and reasonable because when the descending function transitions from a $1/T$ to a $1/T^2$ function at a branch point, the curve is not continuous, causing a jump. This issue does not arise with an oblique straight line, as illustrated in Figure 12. In this figure, curve 1 represents the true acceleration response spectral curve, while curve 2 descends to a $1/T$ function, and curve 3 descends to a $1/T^2$ function. The x-coordinate of the first starting point of descent to a $1/T^2$ function corresponds to the excellent period of the seismic wave, with the y-coordinate at β_{max} , specifically 2.225. In the example of the 1952 Hollywood Storage P.E 270 Deg seismic waves and Appendix 2, it is evident that descending to a $1/T$ function and then to a $1/T^2$ function is inaccurate for almost every β -curve seismic wave. The seismic waves with a real acceleration response greater than $(1/T^2) \cdot \beta_{max}$ in the interval after the

excellent period are listed in Table 1. This analysis confirms that it is not safe to define the second interval function of the descending interval as a $1/T^2$ function. Instead, by descending almost all seismic waves into a $1/T$ function to a branch point and then transitioning to a slope line, as shown in Figure 2, we can safely reflect the true acceleration response.

This problem is not raised by the oblique straight line.

Let's see Fig. 12.

In Fig. 12, curve 1 is the true acceleration response spectral curve and curve 2 is a curve that descends to a $1/T$ function.

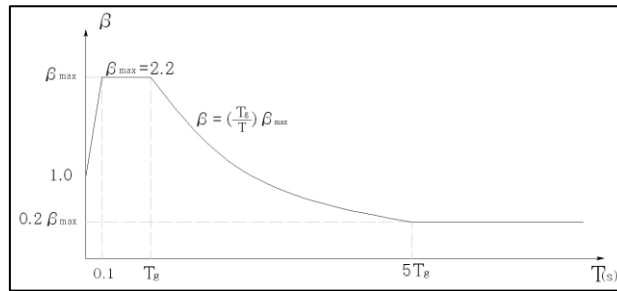


Figure 12 Dynamic coefficient β curve based on the results of the previous study

Curve 3 is a curve that descends to a $1/T^2$ function; the x coordinates of the first starting point, which descended to a $1/T^2$ function descending to a $1/T$ function, are the excellent period points of the corresponding seismic wave, and the y coordinates are β_{max} , in detail, 2.225.

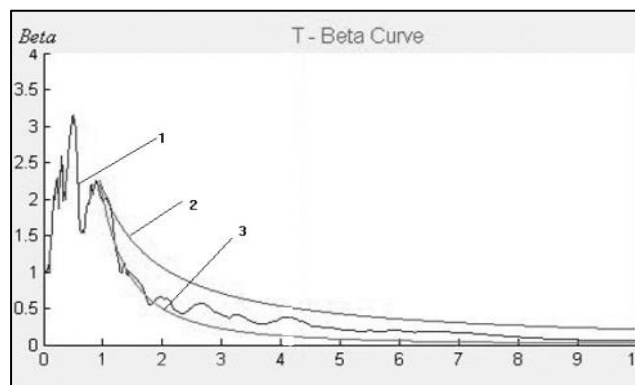


Figure 13 Accelerated response spectral curves of 1952 Hollywood Storage P.E 270

In the 1952 Hollywood Storage P.E 270 Deg seismic waves of the example, and Appendix 2, it can be seen that it is inaccurate to see that it descends to a $1/T$ function to a point of a period at almost every β -curve seismic wave and then descends to a $1/T^2$ function.

The seismic waves with a real acceleration response greater than $(1/T^2) \cdot \beta_{max}$ in the interval after the excellent period are the same as Table 1.

Table 1 The seismic wave with acceleration response greater than $(1/T^2) \cdot \beta_{max}$ in the interval after the excellent period

No	Seismic Waves
1	1940 EL CENTRO Site 270 Deg
2	1940 EL CENTRO Site 180 Deg
3	1952 Taft Lincoln School 69 Deg
4	1952 Taft Lincoln School 339 Deg
5	1952 Hollywood Storage P.E 270 Deg

6	1952 Hollywood Storage P. E 0 Deg
7	1978MIYAGI-Coast, LG
8	1978 MIYAGI-Coast, TR
9	1993 HOKKAIDO-S/W-Coast, LG
10	1968 HYUGANADA-Coast, LG
11	1968 HYUGANADA-Coast, TR
12	1994 HOKKAIDO-EastCoast, TR
13	1983 NIHONKAI-Central, TR
14	1983 NIHONKAI-Central, LG
15	1994 HOKKAIDO-East Coast, LG
16	EL CENTRO, ARRAY6, HUSTON, RD, AT 140 Deg
17	EL CENTRO, ARRAY6, HUSTON, RD, AT 230 Deg
18	HOLLISTER-SOUTH STREET AND PINE DRIVE, AT 0 Deg
19	HOLLISTER-SOUTH STREET AND PINE DRIVE, AT90 Deg
20	NEWHALL-LA COUNTRY FIRE STATION, AT 0 Deg
21	NEWHALL-LA COUNTRY FIRE STATION, AT 90 Deg
22	OAKLAND-OUTER HARBOR WHARF, AT 305Deg
23	T2-I-3 (1995 HYOUGOKEN-South,NS)
24	T2-II-1 (1995 HYOUGOKEN-South,NS)
25	T2-II-2 (1995 HYOUGOKEN-South,EW)
26	T2-III-2 (1995 HYOUGOKEN-South,NS)
27	T2-III-3 (1995 HYOUGOKEN-South,EW)
28	The Chichi(Taiwan) earthquake of September 21, 1999. Unknown recording Station. Longitudinal Component
29	The Chichi(Taiwan) earthquake of September 21, 1999. Unknown recording Station. Transveral Component
30	The Kocaeli(Turkey) Earthquake of August 17, 1999. Sakaria recording Station

Seeing Table 1 and Appendix 2, 30 seismic waves close to nearly half of the 72 seismic waves collected were confirmed that the values of the acceleration response spectra in the period interval up to 10 s currently calculated were significantly greater than the function values of $1/T^2$.

The remaining 42 seismic waves were found to be very close to the $1/T^2$ function values in a relatively long period, but by no means less than $1/T^2$ the value of the acceleration response spectrum.

Therefore, we can conclude that it is not safe to catch the second interval function of the descending interval as a $1/T^2$ function.

In Appendix 2, it is concluded that by descending almost all seismic waves into a function of $1/T$ to a branch point and then taking a descending function in a slope line, as shown in Figure 2, we can safely reflect the true state of the acceleration response. Here, the lower limit value of the dynamic coefficient β curve is determined statistically from the calculated results when $T = 10$ seconds. The finishing period of foreign aseismic standards is usually between 3 to 4 seconds, and considering a period of 6 seconds along with the natural vibration period calculation results of actual structures, we can utilize the values of the dynamic coefficients in real and scientific research. The value of the acceleration response spectrum when $T = 10$ seconds is expressed as a ratio of β_{max} , rather than an absolute value. The mean value of the acceleration response spectrum at 72 seismic waves at $T = 10$ seconds is 0.08632, with a standard deviation of 0.1325, and $0.0388\beta_{max}$, with a standard deviation of $0.05956\beta_{max}$. The detailed calculation results are presented in Appendix 1. Now, let us estimate the value of the lower limit with a 95% confidence rate, similar to the estimation of β_{max} . The confidence interval of the lower limit value of the acceleration response spectrum is estimated as follows with a 95% confidence rate: $(0.05294\beta_{max} \sim 0.02467\beta_{max})$. Thus, from a safety perspective, the lower limit value is $0.05294\beta_{max}$. Since the branching point value is 5.5 Tg, we take the descending shape into the slope line

after the bifurcation point as follows: $\beta = [a - b(T - 5.5T_g)] \cdot \beta_{max}$. By substituting the boundary conditions when $T = 5.5 T_g$ and $T = 10$ seconds, and considering T_g to be 0.1 seconds for safety, we determine the values of a and b in Equation 18 to be 0.18 and 0.0135, respectively. The result is equal to Equation 19: $\beta = [0.18 - 0.0135(T - 5.5T_g)] \cdot \beta_{max}$. Thus, finally, the dynamic coefficient β is determined as shown in Figure 14, with β_{max} being 2.2, as previously established.

The confidence interval of the lower limit value of the acceleration response spectrum is estimated as follows with 95% confidence rate.

$$(0.0388 - 1.96 \cdot \frac{0.05956}{\sqrt{71}}, 0.0388 + 1.96 \cdot \frac{0.05956}{\sqrt{71}}) \beta_{max}$$

$$= (0.02467 \sim 0.05294) \beta_{max}$$

Thus, from the point of view of safety, the lower limit value is $0.05294\beta_{max}$.

Since the branching point value is $5.5 T_g$, let's take the descending shape into the slope line after the bifurcation point as follows.

$$\beta = [a - b(T - 5.5T_g)] \cdot \beta_{max} \tag{24}$$

If we look at Equation 18, we need to obtain a, b by substituting the boundary conditions when $T = 5.5 T_g$ and when $T = 10$ s.

By the way, T_g is unknown.

The smaller the value of T_g , the safer the value of b .

Therefore, we determined the value of T_g to be 0.1 s which could be the lowest and the a and b of Equation 18 to 0.18 and 0.0135, respectively.

The result is equal to Equation 19.

$$\beta = [0.18 - 0.0135(T - 5.5T_g)] \cdot \beta_{max} \tag{25}$$

Thus, finally, the dynamical coefficient β is determined as Fig. 14.

β_{max} is 2.2, as we have seen before.

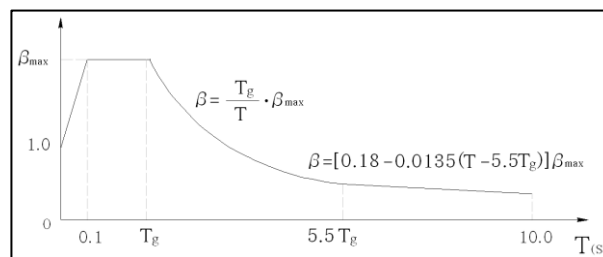


Figure 14 The newly proposed dynamical coefficient β curve

4. Conclusions

Based on the insights gained from this study, we conclude that representing the acceleration response as a multiple of β_{max} when $T = 0$ is inaccurate; instead, it is correct to represent β as 1.0. The dynamic coefficient curve, which descends to a $1/T$ fractional function and then transitions into an oblique straight line, is scientifically robust and offers superior safety compared to descending to a $1/T^2$ function. This approach provides a more accurate representation of the acceleration response, particularly for structures with longer natural vibration periods. In determining the excellent period of seismic waves, it is argued that this can be achieved more precisely by combining acceleration response spectral values rather than relying solely on Fourier spectral values. The proposed dynamic coefficient curve, as illustrated in Figure 13, is both scientific and reliable, serving as a solid foundation for elastic response spectral analysis and demand spectrum

methodologies, particularly in the context of buildings with relatively large natural vibration periods. This study contributes to enhancing the accuracy and applicability of seismic design standards, ensuring improved structural resilience against seismic forces.

5. Acknowledgements

We would like to express our sincere gratitude to the Faculty of Civil Engineering at Pyongyang University of Architecture for their support and resources, which were instrumental in conducting this research. We also extend our appreciation to our colleagues and collaborators who provided valuable insights and feedback throughout the study. Special thanks to the technical staff for their assistance in data collection and analysis. Additionally, we acknowledge the constructive comments from the reviewers, which helped improve the quality of this manuscript.

6. Conflict of Interest

The authors declare that there are no conflicts of interest regarding the publication of this paper. All authors have approved the final version of the manuscript and agree with its submission to the International Journal of Architecture and Urbanism.

Reference

- [1] Song Chon Choi (2010), The Aseismic Structural Design Standards for Building, The Ministry of Management of State Construction: 20–32
- [2] GB 5011-2010(2010), Building Aseismic Design Code, Unity Training Course, Earthquake Press: 51–65
- [3] Tan Wenhui and Li Da, High-rise building structure design, YeJin Industrial press 2013. 80–90
- [4] E. Kurbatsky dan V. Mondrus, "Dynamic Coefficients or Response Spectra of Structures to Earthquake?," Scientific journal "ACADEMIA. ARCHITECTURE AND CONSTRUCTION", vol. 2019, 2019. [Online].
- [5] M. Pehlivan, E. Rathje, dan R. Gilbert, "Factors influencing soil surface seismic hazard curves," Soil Dynamics and Earthquake Engineering, vol. 83, pp. 180-190, 2016. [Online].
- [6] F. Behnamfar dan A. Fathollahi, "Conversion factors for design spectral accelerations including soil–structure interaction," Bulletin of Earthquake Engineering, vol. 14, pp. 2731-2755, 2016. [Online].
- [7] M. Al-Ansari, "Reliability Index of Tall Buildings in Earthquake Zones," OJER, vol. 2, no. 3, pp. 39-46, 2013. [Online].
- [8] F. Sardari, M. R. Dehkordi, M. Eghbali, dan D. Samadian, "Practical seismic retrofit strategy based on reliability and resiliency analysis for typical existing steel school buildings in Iran," International Journal of Disaster Risk Reduction, vol. 51, pp. 101890, 2020. [Online].
- [9] N. Lagaros, A. Th. Garavelas, dan M. Papadrakakis, "Innovative seismic design optimization with reliability constraints," Computer Methods in Applied Mechanics and Engineering, vol. 198, pp. 28-41, 2008. [Online].
- [10] C. Fang dan W. Wang, "Structural Responses: Single-Degree-of-Freedom (SDOF) Systems," Shape Memory Alloys for Seismic Resilience, Springer, 2019. [Online].
- [11] E. Bojórquez, J. Bojórquez, S. Ruiz, A. Reyes-Salazar, dan J. I. Velazquez-Dimas, "Response transformation factors for deterministic-based and reliability-based seismic design," Structural Engineering and Mechanics, vol. 46, no. 6, pp. 755-773, 2013. [Online].
- [12] F. Graziotti, A. Penna, dan G. Magenes, "A nonlinear SDOF model for the simplified evaluation of the displacement demand of low-rise URM buildings," Bulletin of Earthquake Engineering, vol. 14, no. 6, pp. 1589-1612, 2016. [Online].
- [13] J. Karapetyan, "Comparative analysis of dynamic coefficient $\beta(T, n)$ curves obtained by different methods," Seismic Instruments, vol. 49, pp. 307-314, 2013. [Online]. Available: https://consensus.app/papers/analysis-coefficient-curves-obtained-methods-karapetyan/f61ec172708e5a74b3fa928147d5a40e/?utm_source=chatgpt.
- [14] K. Kawashima dan K. Aizawa, "MODIFICATION OF EARTHQUAKE RESPONSE SPECTRA WITH RESPECT TO DAMPING," Doboku Gakkai Ronbunshu, vol. 1984, pp. 351-355, 1984. [Online]. Available: https://consensus.app/papers/modification-earthquake-response-spectra-with-respect-kawashima/8509eadc8ab05cd482a59e1b108e1538/?utm_source=chatgpt.

- [15] Z. Yongfeng dan T. Gengshu, "An Investigation of Characteristic Periods of Seismic Ground Motions," Journal of Earthquake Engineering, vol. 13, pp. 540-565, 2009. [Online]. Available: https://consensus.app/papers/investigation-characteristic-periods-seismic-ground-yongfeng/3762dd2ed3cb52f0b7fb557424b533c3/?utm_source=chatgpt.
- [16] G. Chen, X. Ning, H. Guo, dan H. Zhou, "Characteristic Analysis of 3.11 Seismic Waves," Advanced Materials Research, vol. 838-841, pp. 1484-1491, 2013. [Online]. Available: https://consensus.app/papers/analysis-seismic-waves-chen/8b69aad6e23b5b748729205a9a5e6f11/?utm_source=chatgpt.
- [17] Q. Bai, F. Zhu, Y. Kang, dan J. Bian, "Power spectral density estimation of seismic wave based on wavelet transform," 2008 Chinese Control and Decision Conference, pp. 4600-4603, 2008. [Online]. Available: https://consensus.app/papers/power-density-estimation-wave-based-wavelet-transform-bai/d822565c3e3d51cc8e8beabda8897e670/?utm_source=chatgpt.

Appendix 1

Table Characteristics of seismic acceleration records

No	Seismic Wave	Maximum acceleration peak value	Appearance Time(s)	Continuance Time(s)	excellent period Tg(s)	$\beta(10s)$
1	1940 EL CENTRO Site 270 Deg	-0.356g	2.14	53.72	0.68	0.0455
2	1940 EL CENTRO Site 180 Deg	0.214g	11.46	53.46	0.4689	0.1155
3	1952 Taft Lincoln School 69 Deg	-0.155g	9.12	54.38	0.7251	0.03573
4	1952 Taft Lincoln School 339 Deg	0.1793g	3.72	54.40	0.3358	0.06536
5	1952 Hollywood Storage P.E 270 Deg	0.0592g	13.32	78.62	0.9472	0.06157
6	1952 Hollywood Storage P. E 0 Deg	-0.042g	13.0	78.62	0.8364	0.1228
7	1971 San Fernando 69 Deg	0.3154g	2.62	61.84	0.3398	0.01652
8	1971 San Fernando 159 Deg	0.2706g	1.92	61.88	0.4653	0.04022
9	1979 James RD EL CENTRO 220 Deg	0.7777g	6.78	37.68	0.628	0.01491
10	1979 James RD EL CENTRO 310 Deg	-0.595g	7.82	37.82	0.7136	0.02261
11	1994 Northridge Sylmar Country Hosp 90 Deg	0.6038g	4.08	59.98	0.6316	0.01785
12	1994 Northridge, Arleta and Nordthoff Fire Station 90 Deg	0.3437g	3.60	59.98	0.9231	0.0216
13	1989 Loma Prieta, Oakland Outer Wharf 270 Deg	0.2755g	12.60	39.98	0.5882	0.01812
14	1989 Loma Prieta, Oakland Outer Wharf 0 Deg	-0.219g	12.68	39.98	0.7692	0.02226
15	1971 San Fernando POCOIMA Dam 196 Deg	1.0748g	8.50	41.58	0.4289	0.00705
16	1971 San Fernando POCOIMA Dam 286 Deg	-1.169g	7.74	41.74	0.2091	0.02454
17	1966 Parkfield Cholame Shandon 40 Deg	-0.237g	4.64	26.06	0.4742	0.01942
18	1966 Parkfield Cholame Shandon 130 Deg	-0.274g	4.54	26.06	0.4921	0.01174
19	1978MIYAGI-Coast, LG	0.3251g	2.27	30	1.3636	0.29682
20	1978 MIYAGI-Coast, TR	0.3262g	9.05	30	1.1111	0.34515
21	1993 HOKKAIDO-S/W-Coast, LG	-0.329g	20.91	40	1.5385	0.3297
22	1968 HYUGANADA-Coast, LG	-0.369g	17.79	40	1.3333	0.23598
23	1968 HYUGANADA-Coast, TR	0.3925g	15.88	40	1.1765	0.31154
24	1994 HOKKAIDO-East Coast, TR	-0.372g	29.96	65	1.0656	0.31509
25	1983 NIHONKAI-Central, TR	-0.441g	41.38	60	1.7647	0.35036
26	1983 NIHONKAI-Central, LG	-0.432g	32.98	60	1.6216	0.46756
27	1994 HOKKAIDO-East Coast, LG	0.4471g	20.76	60	2.1429	0.76077
28	1995 HYOGOKEN-South, NS	-0.828g	5.54	30	0.7317	0.02305
29	1995 HYOGOKEN-South, EW	0.781g	8.87	30	0.5357	0.03002
30	1995 HYOGOKEN-South, N30W	0.7509g	4.98	40	1.3333	0.05154
31	1995 HYOGOKEN-South, N12W	-0.602g	6.30	50	1.5152	0.09579
32	ALTADENA-EATION CANYON PARK AT 0 Deg	-438.913gal	2.86	40	0.4211	0.00221
33	ALTADENA-EATION CANYON PARK AT 90 Deg	175.617gal	3.16	40	0.4598	0.00336
34	EL CENTRO, ARRAY6, HUSTON, RD, AT 140 Deg	-368.67gal	2.48	39.09	0.8317	0.04506
35	EL CENTRO, ARRA Y6, HUSTON, RD, AT 230 Deg	-428.09gal	5.95	39.12	0.9093	0.0777
36	CORRALITOS-EUR EKA CANYON, RD, AT 0	617.695	2.62	40.16	0.7146	0.01206

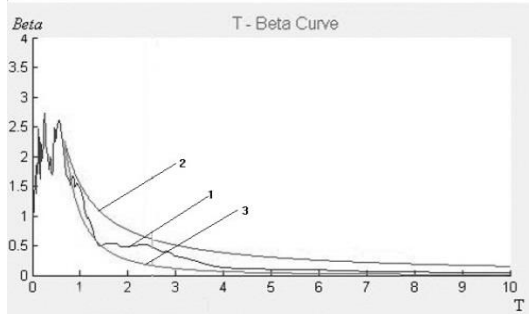
	Deg	gal				
37	CORRALITOS-EUR EKA CANYON, RD, AT 90 Deg	469.384 gal	4.06	40	0.7547	0.01957
38	HOLLISTER-SOUTH STREET AND PINE DRIVE AT 0 Deg	361.90 gal	8.50	60	0.9677	0.05621
39	HOLLISTER-SOUTH STREET AND PINE DRIVE AT 90 Deg	-174.549gal	7.34	60.16	0.5456	0.10729
40	CENTURY CITY-LACC NORTH AT 0 Deg	217.296 gal	8.94	60	0.8955	0.01358
41	CENTURY CITY-LACC NORTH AT 90 Deg	250.667 gal	6.84	60	0.6	0.0175
42	LEXINGTON DAM AT 0 Deg	-433.563gal	4.20	40	1.1111	0.02269
43	LEXINGTON DAM AT 90 Deg	-401.641gal	4.06	40	1.0811	0.03347
44	NEWHALL-LA COUNTRY FIRE STATION AT 0 Deg	578.19gal	4.34	60	0.6977	0.03476
45	NEWHALL-LA COUNTRY FIRE STATION AT 90 Deg	-571.62gal	5.36	60	0.5769	0.0171
46	OAKLAND-OUTER HARBOR WHARF AT 35 Deg	281.37 gal	13.48	40	0.9524	0.01853
47	OAKLAND-OUTER HARBOR WHARF AT 305Deg	265.5gal	12.70	40	1.5385	0.02065
48	PETROLIA AT 0 Deg	-578.1 gal	3.44	60	0.7407	0.01781
49	PETROLIA AT 90 Deg	649.44 gal	3.30	60	0.8108	0.02223
50	POMONA-4TH & LOCUST AT 0 Deg	-182.16 gal	3.48	40	0.396	0.00439
51	POMONA-4TH & LOCUST AT 90 Deg	203.034 gal	3.52	40	0.1338	0.0037
52	SANTA MONICA-CITY HALL GROUNDS AT 0 Deg	-362.618gal	9.92	60	0.3727	0.01172
53	SANTA MONICA-CITY HALL GROUNDS AT 90 Deg	-865.965gal	9.82	60	0.22734	0.01046
54	SYLMAR-COUNTY HOSP PARKING LOT AT 0 Deg	826.76gal	4.22	60	0.5085	0.01172
55	SYLMAR-COUNTY HOSP PARKING LOT AT 90 Deg	592.64gal	4.10	60	0.8571	0.02384
56	YERMO-FIRE STATION AT 0 Deg	-148.57 gal	14.84	80	1.4286	0.14135
57	YERMO-FIRE STATION AT 90 Deg	-240.02 gal	16.34	80	1.3793	0.15621
58	Taft (1952)	291.7gal	6.74	7.98	0.4444	0.01293
59	EL CENTRO(1940)	341.7gal	2.12	4.58	0.57143	0.02036
60	Ning He	200gal	0.94	10.98	0.8462	0.07225
61	Qian an	-200gal	1.50	4.58	0.2421	0.00791
62	T2-I-3 (1995 HYOUGOKEN-South, NS)	0.7955g	8.96	30	0.6818	0.02815
63	T2-II-1 (1995 HYOUGOKEN-South, NS)	0.7005g	8.48	40	1.0256	0.05069
64	T2-II-2 (1995 HYOUGOKEN-South,EW)	-0.6859g	7	40	1.0811	0.07183
65	T2-III-2 (1995 HYOUGOKEN-South, NS)	-0.5685g	6.2	50	1.6667	0.10585
66	T2-III-3 (1995 HYOUGOKEN-South, EW)	0.6314g	6.14	50	1.6667	0.0951
67	The Chichi(Taiwan) earthquake of September 21, 1999. Unknown recording Station. Longitudinal Component	0.8082g	14.31	40	0.5884	0.29042
68	The Chichi(Taiwan) earthquake of September 21, 1999. Unknown recording Station. Transveral Component	0.8531g	14.67	40	0.5872	0.2074
69	The Loma Prieta (USA)earthquake of October 18, 1989. Corralitos recording Station	0.7992g	3.96	16.9	0.7357	0.0144
70	The Loma Prieta (USA)earthquake of October 18, 1998. Emeryville recording Station	0.2498g	5.56	20.53	1.4671	0.02184
71	The Friulli(Italy) Earthquake of May 6, 1976. Unknown recording Station	0.4788g	4.02	20	0.5002	0.01079

72	The Hollister(USA) Earthquake of November 28, 1974. City Hall recording Station	0.12g	1.85	15.06	0.3076	0.00584
----	---	-------	------	-------	--------	---------

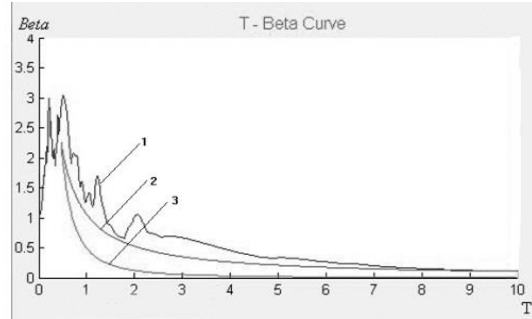
$1g=9.81m/s^2=981gal$, $1gal=1cm/s^2=0.01m/s^2$

Appendix 2

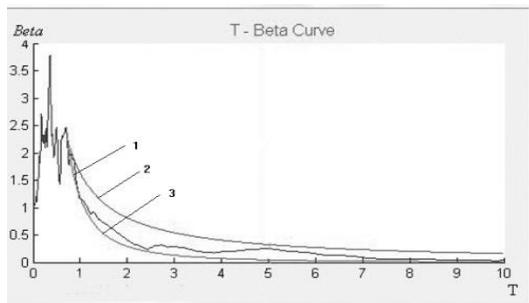
In the figures of Appendix 2, curve 1 is the acceleration response spectral curve, curve 2 is a curve that descends to a $1/T$ function, and curve 3 is a curve that descends to a $1/T^2$ function.



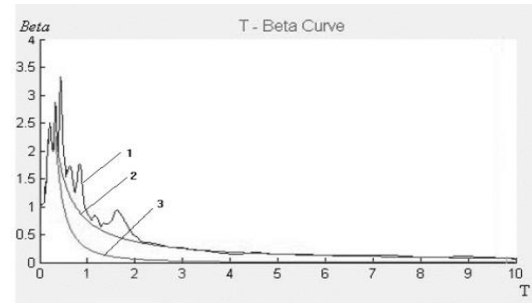
1. 1940 EL CENTRO Site 270 Deg



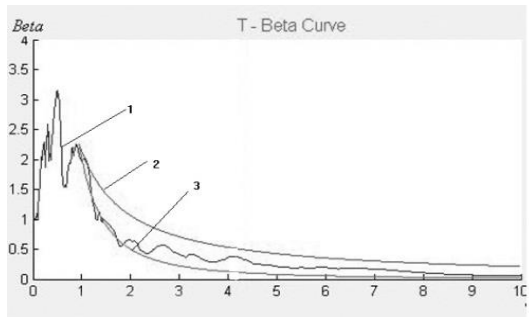
2. 1940 EL CENTRO Site 180 Deg



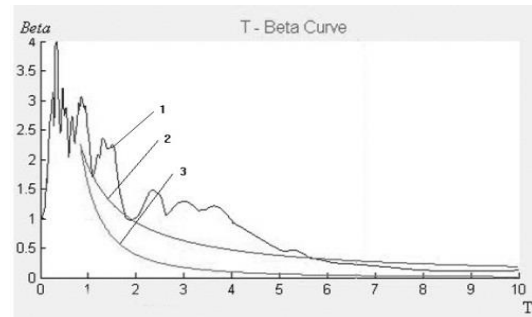
3. 1952 Taft Lincoln School 69 Deg



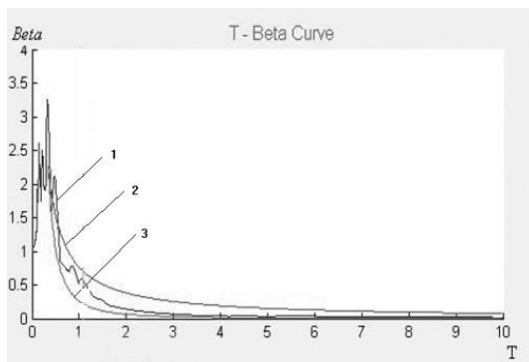
4. 1952 Taft Lincoln School 339 Deg



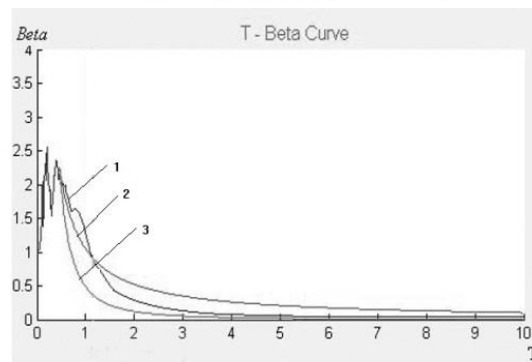
5. 1952 Hollywood Storage P.E 270 Deg



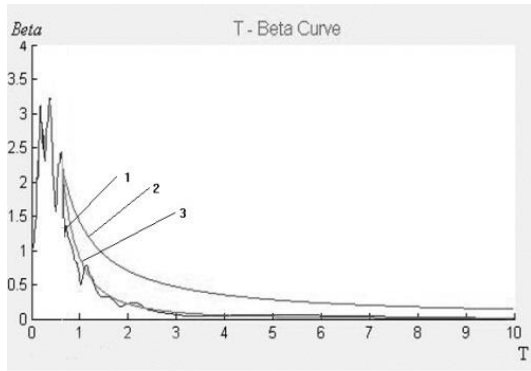
6. 1952 Hollywood Storage P. E 0 Deg



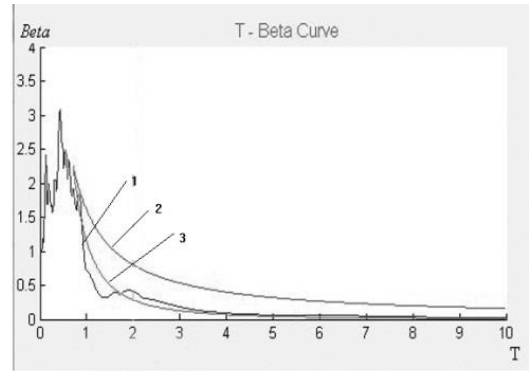
7. 1952 Hollywood Storage P. E 0 Deg



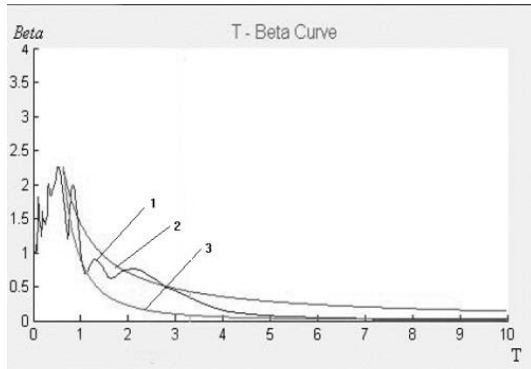
8. 1971 San Fernando 159 Deg



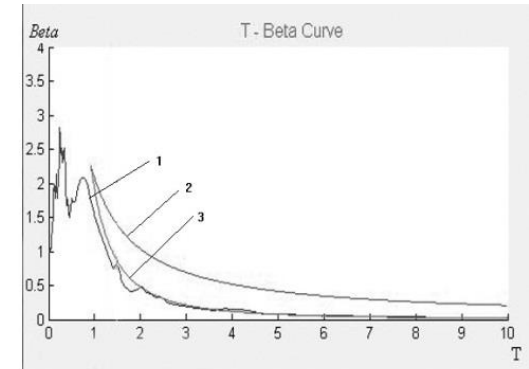
9. 1979 James RD EL CENTRO 220 Deg



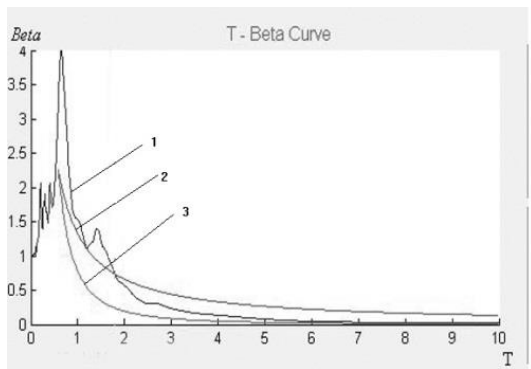
10. 1979 James RD EL CENTRO 310 Deg



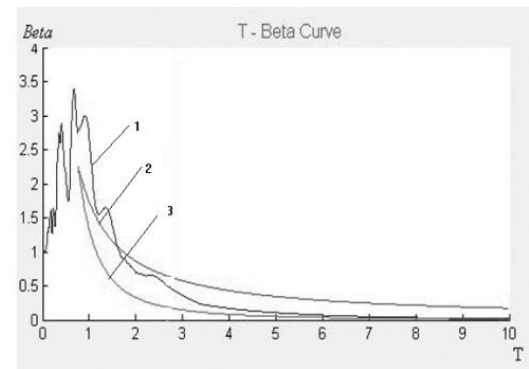
11. 1994 Northridge Sylmar Country Hosp 90 Deg



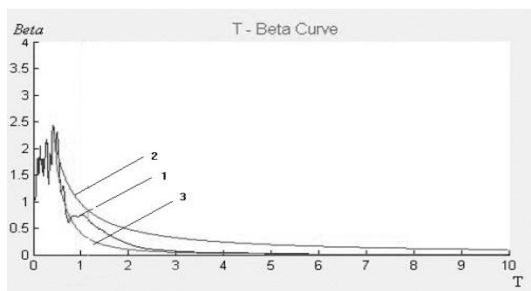
12. 1994 Northridge, Arleta and Nordthoff Fire Station 90 Deg



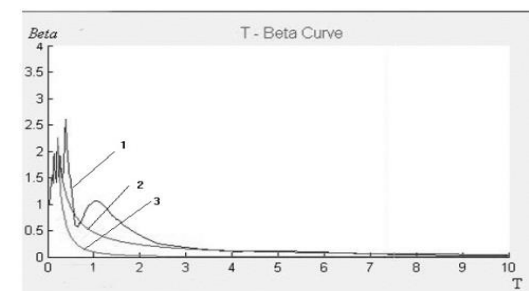
13. 1989 Loma Prieta, Oakland Outer Wharf 270 Deg



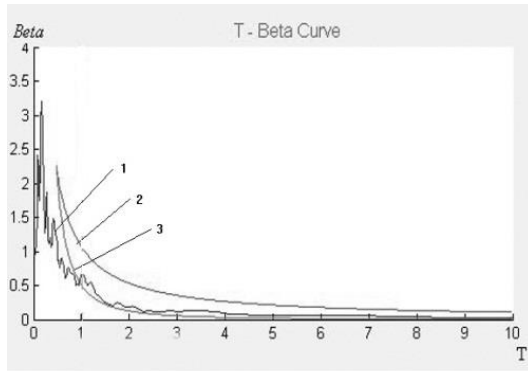
14. 1989 Loma Prieta, Oakland Outer Wharf 0 Deg



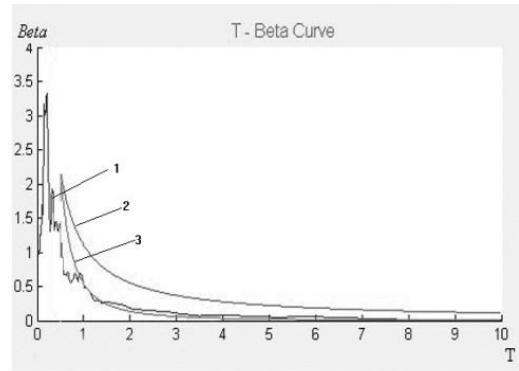
15. 1971 San Fernando POCOIMA Dam 196 Deg



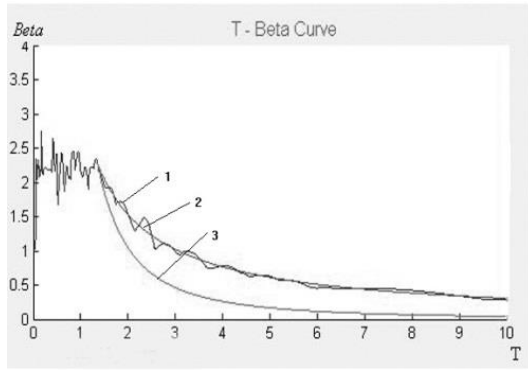
16. 1971 San Fernando POCOIMA Dam 286 Deg



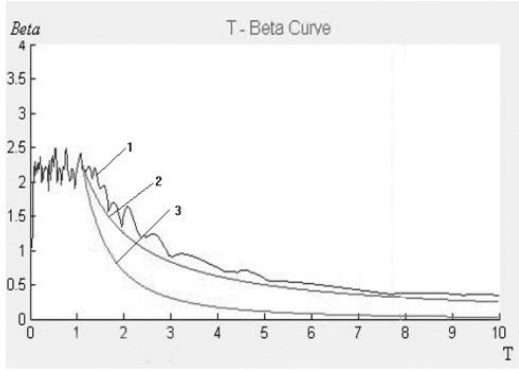
17. 1966 Parkfield Cholame Shandon 40 Deg



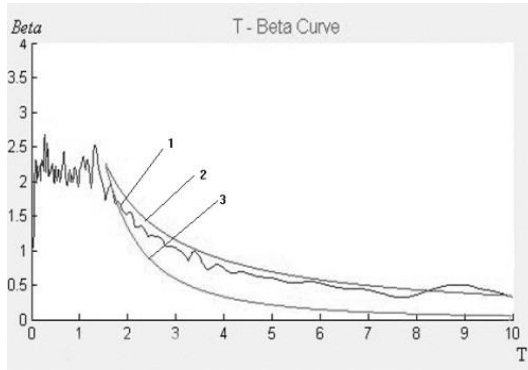
18. 1966 Parkfield Cholame Shandon 130 Deg



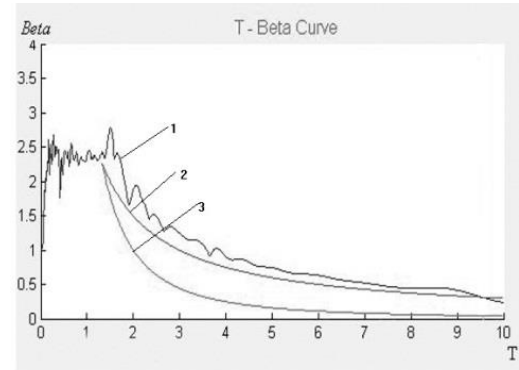
19. 1978 MIYAGI-Coast, LG



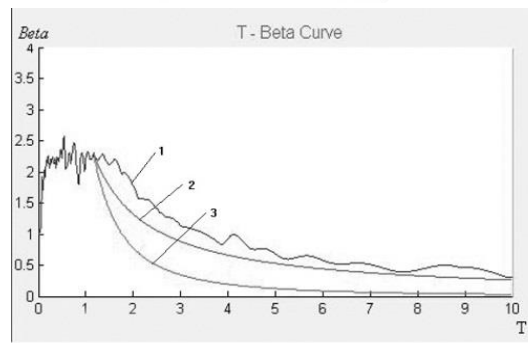
20. 1978 MIYAGI-Coast, TR



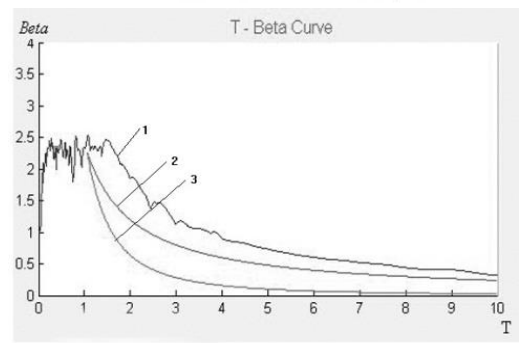
21. 1993 HOKKAIDO-S/W-Coast, LG



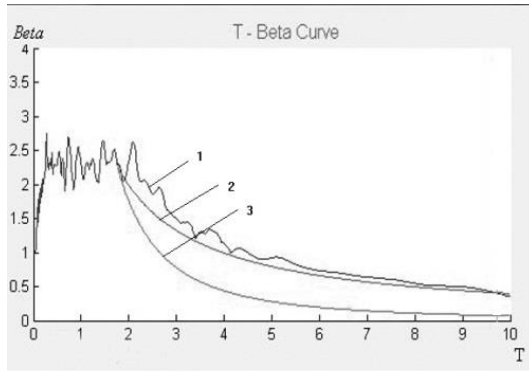
22. 1968 HYUGANADA-Coast, LG



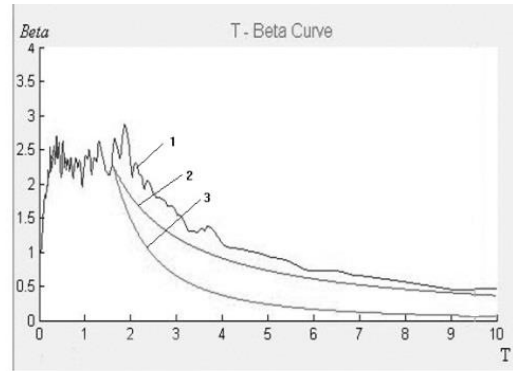
23. 1968 HYUGANADA-Coast, TR



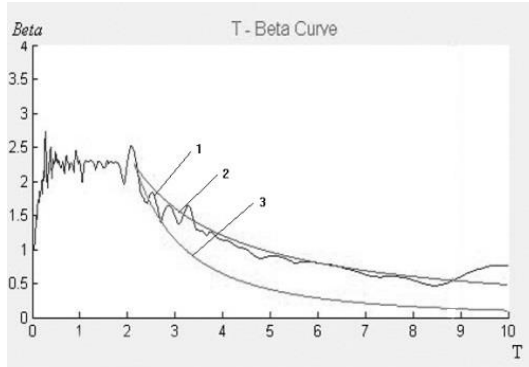
24. 1994 HOKKAIDO-East Coast, TR



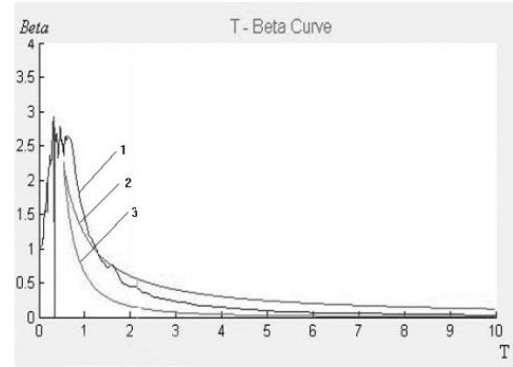
25. 1983 NIHONKAI-Central, TR



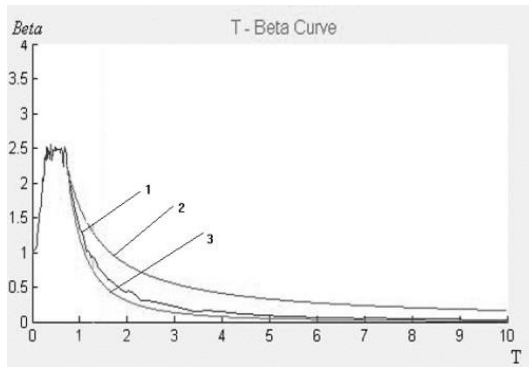
26. 1983 NIHONKAI-Central, LG



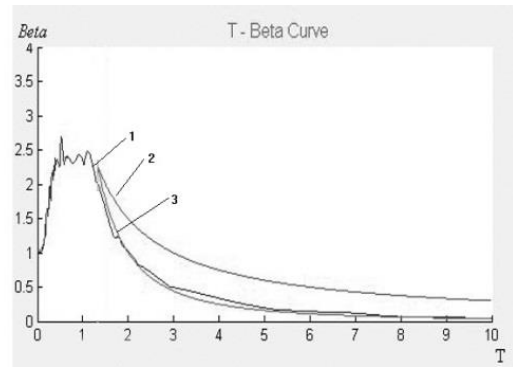
27. 1994 HOKKAIDO-East Coast, LG



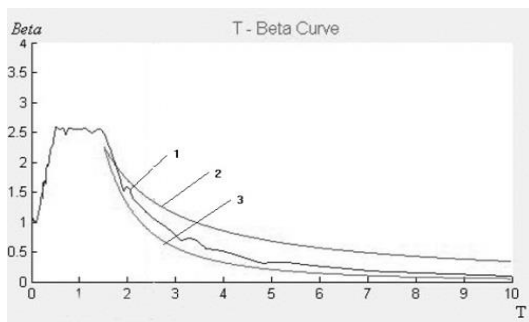
28. 1995 HYOGOKEN-South, NS



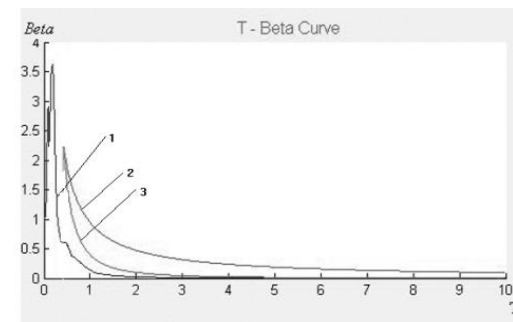
29. 1995 HYOGOKEN-South, EW



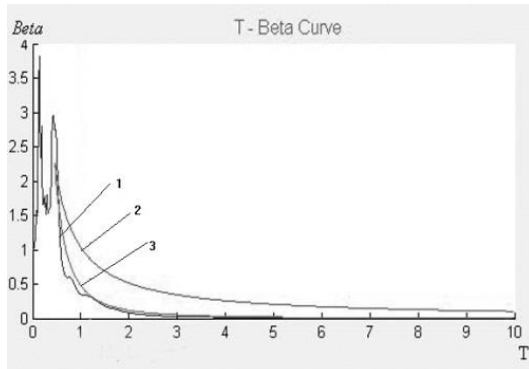
30. 1995 HYOGOKEN-South, N30W



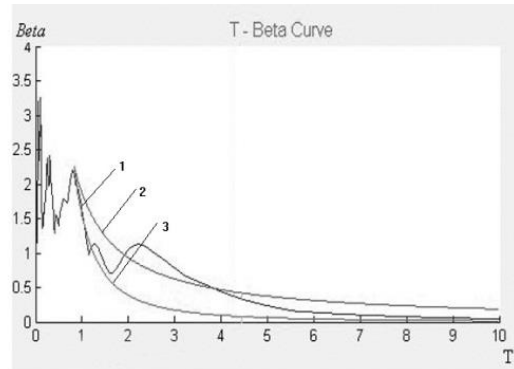
31. 1995 HYOGOKEN-South, N12W



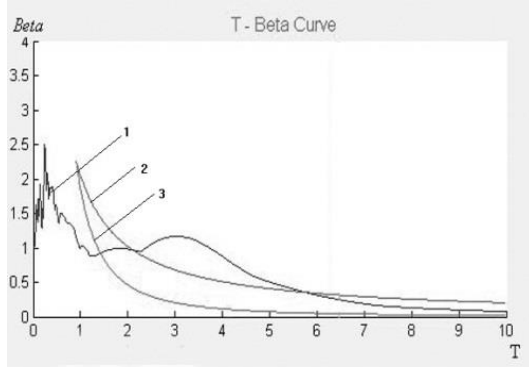
32. ALTADENA-EATION CANYON PARK AT 0 Deg



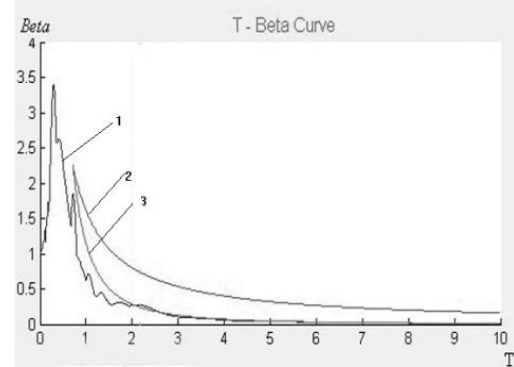
33. ALTADENA-EATION CANYON PARK AT 90 Deg



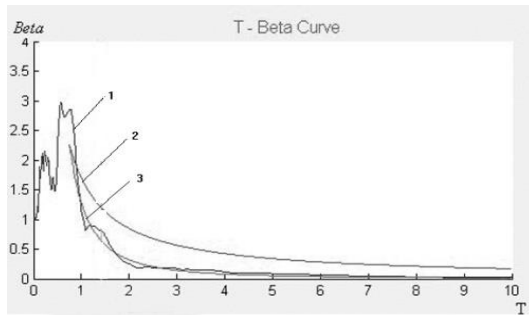
34. EL CENTRO, ARRAY6, HUSTON, RD, AT



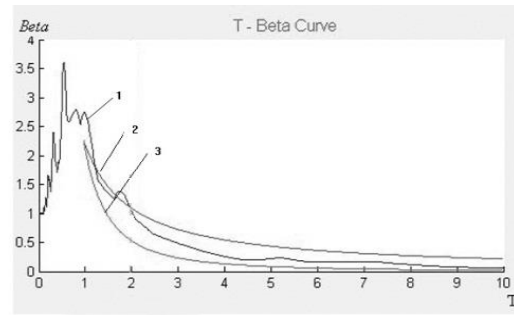
35. EL CENTRO, ARRA Y6, HUSTON, RD, AT 230 Deg



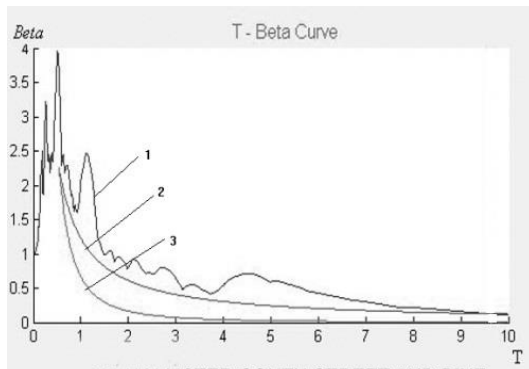
36. CORRALITOS-EUR EKA CANYON, RD, AT 0 Deg



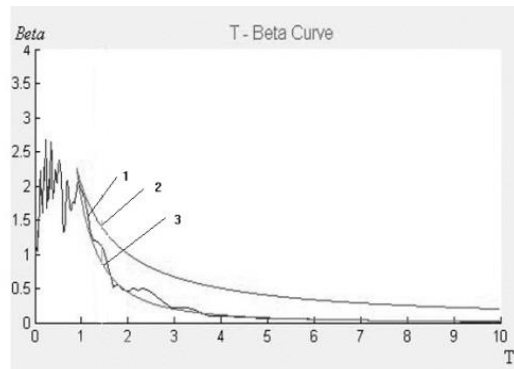
37. CORRALITOS-EUR EKA CANYON, RD, AT 90 Deg



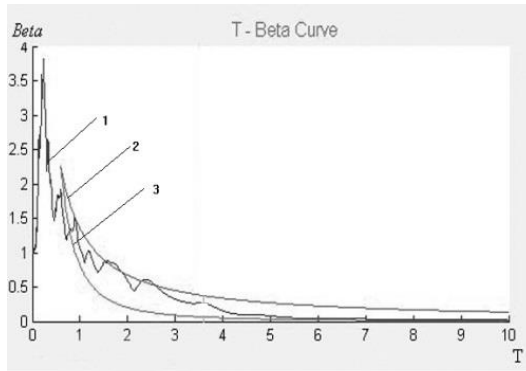
38. HOLLISTER-SOUTH STREET AND PINE DRIVE AT 0 Deg



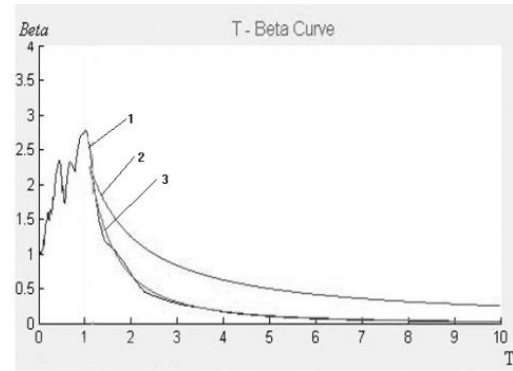
39. HOLLISTER-SOUTH STREET AND PINE DRIVE AT 90 Deg



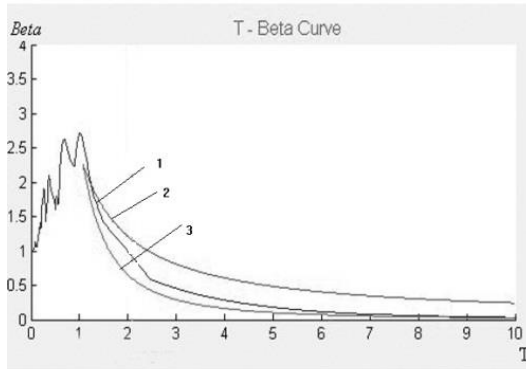
40. CENTURY CITY-LACC NORTH AT 0 Deg



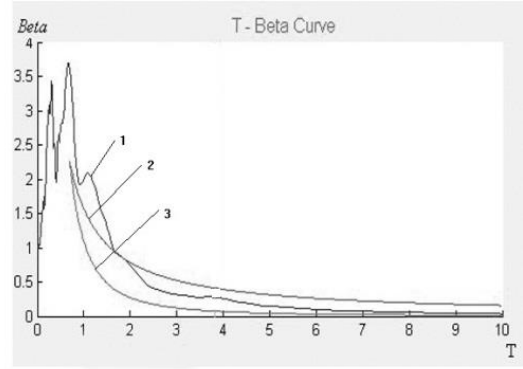
41. CENTURY CITY-LACC NORTH AT 90 Deg



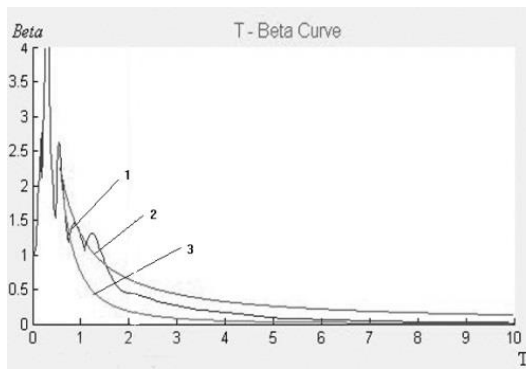
42. LEXINGTON DAM AT 0 Deg



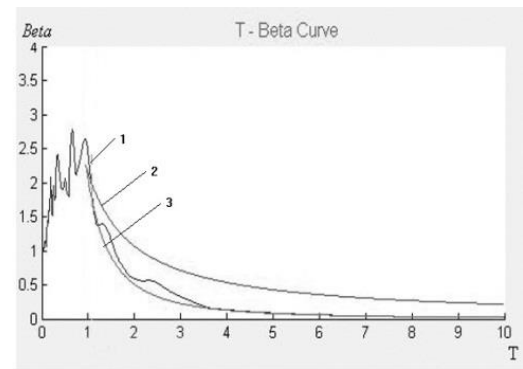
43. LEXINGTON DAM AT 90 Deg



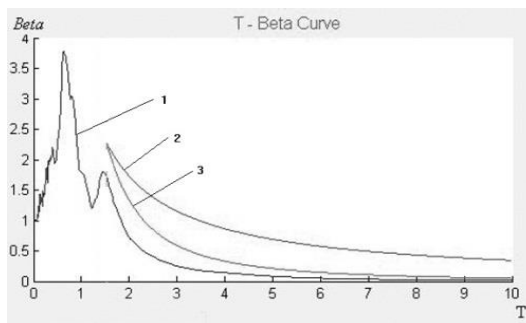
44. NEWHALL-LA COUNTRY FIRE STATION AT 0 Deg



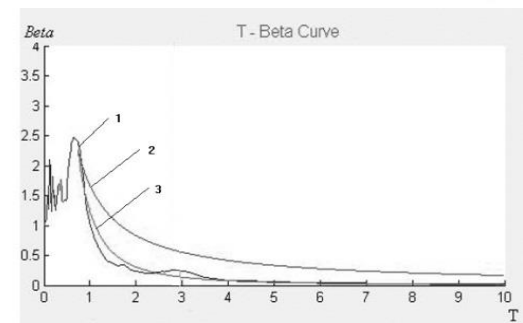
45. NEWHALL-LA COUNTRY FIRE STATION AT 90 Deg



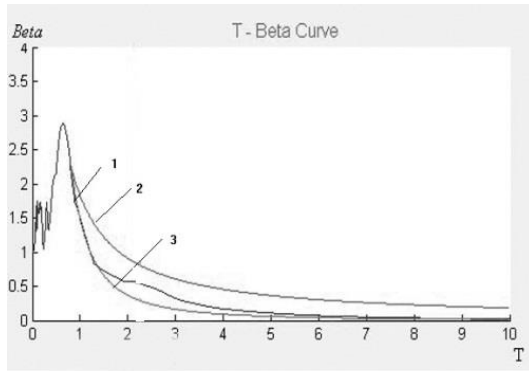
46. OAKLAND-OUTER HARBOR WHARF AT 35 Deg



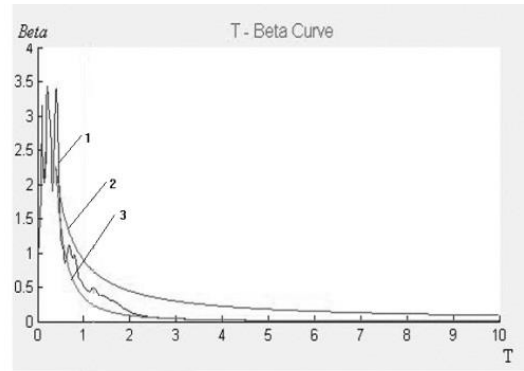
47. OAKLAND-OUTER HARBOR WHARF AT 305 Deg



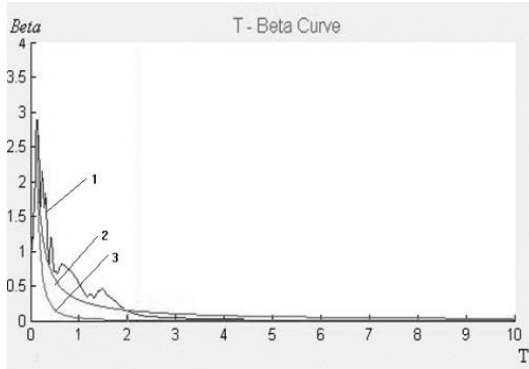
48. PETROLIA AT 0 Deg



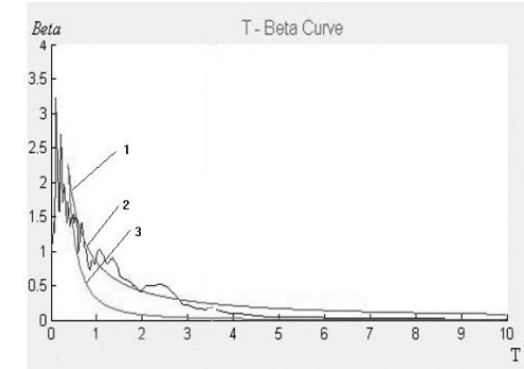
49. PETROLIA AT 90 Deg



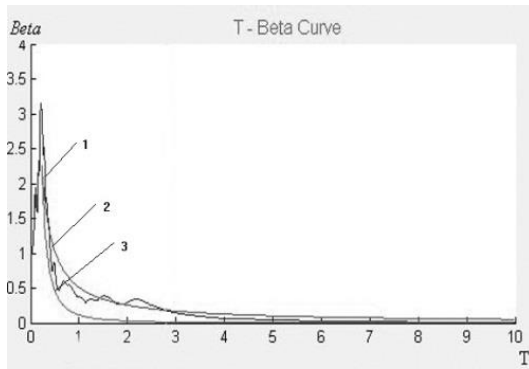
50. POMONA-4TH & LOCUST AT 0 Deg



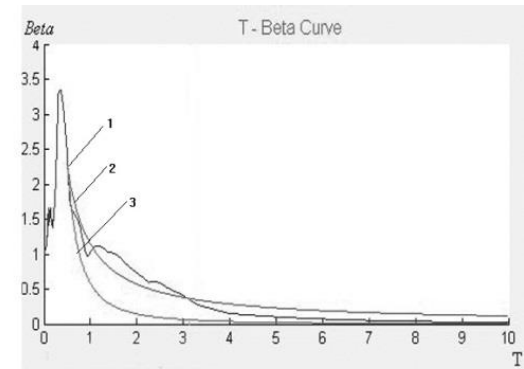
51. POMONA-4TH & LOCUST AT 90 Deg



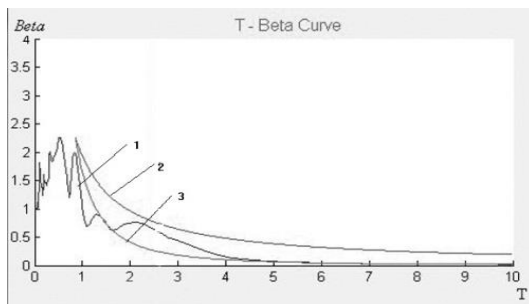
52. SANTA MONICA-CITY HALL GROUNDS AT 0 Deg



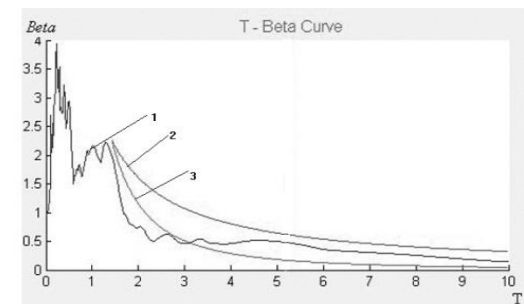
53. SANTA MONICA-CITY HALL GROUNDS AT 90 Deg



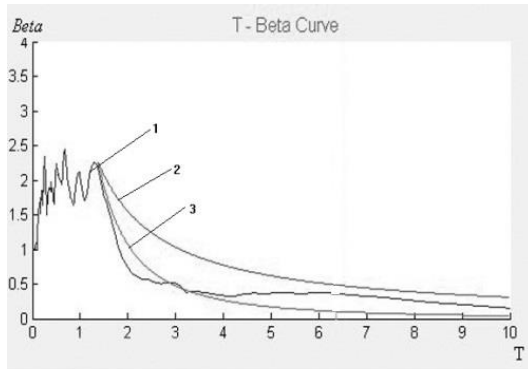
54. SYLMAR-COUNTY HOSP PARKING LOT AT 0 Deg



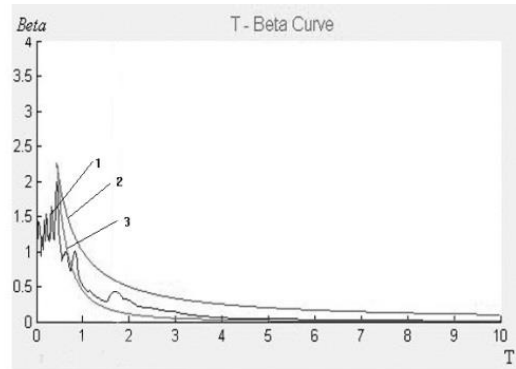
55. SYLMAR-COUNTY HOSP PARKING LOT AT 90 Deg



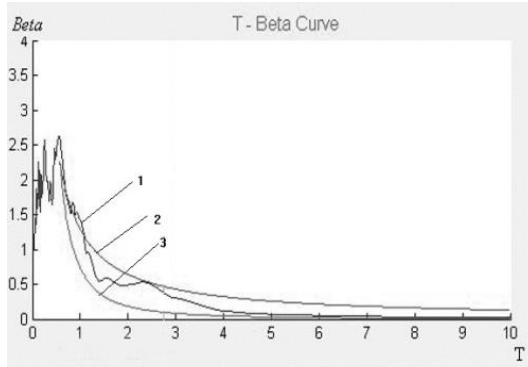
56. YERMO-FIRE STATION AT 0 Deg



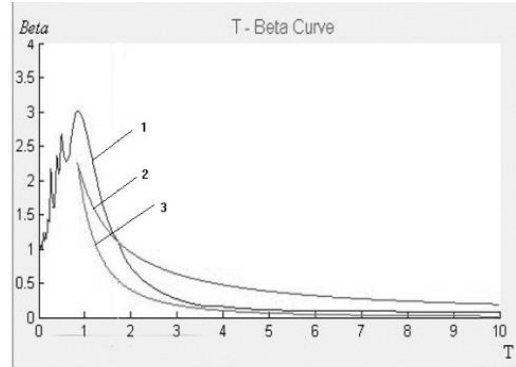
57. YERMO-FIRE STATION AT 90 Deg



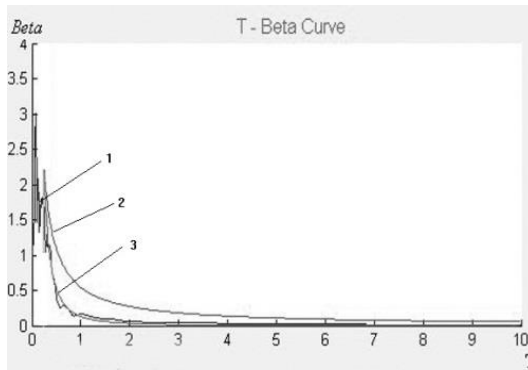
58. Taft (1952)



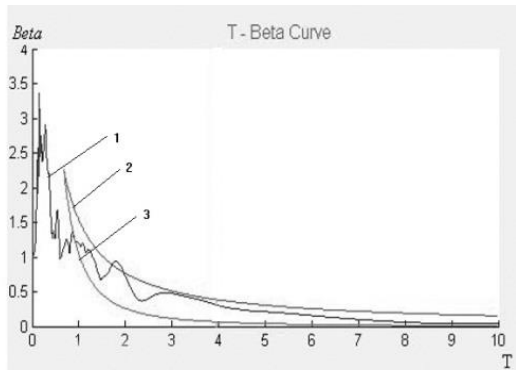
59. EL CENTRO (1940)



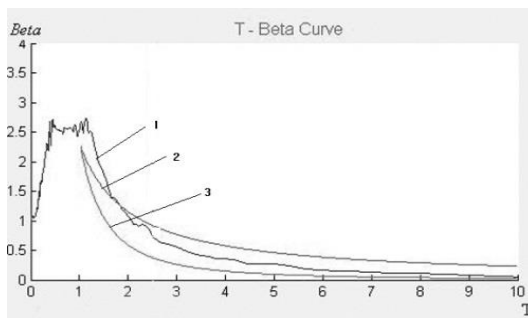
60. Ning He



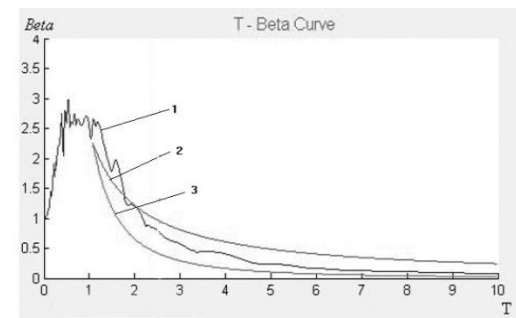
61. Qian an



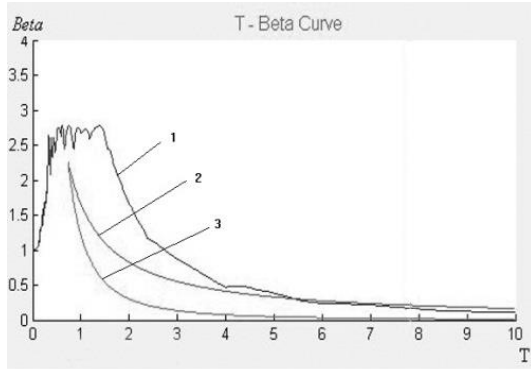
62. T2- 1-3 (1995 HYUGOKEN-South,NS)



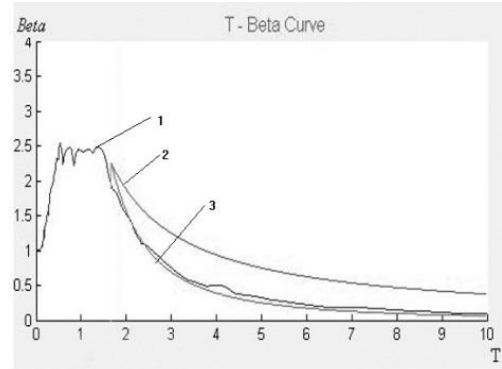
63. T2- 2-1 (1995 HYUGOKEN-South,NS)



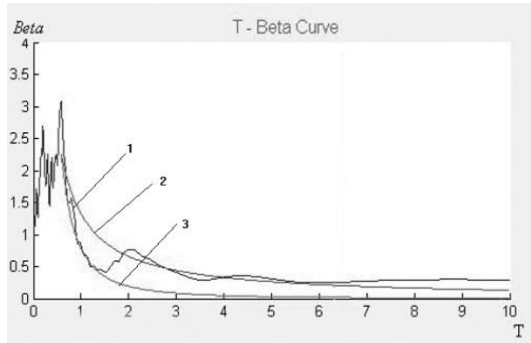
64. T2- 2-2 (1995 HYUGOKEN-South,EW)



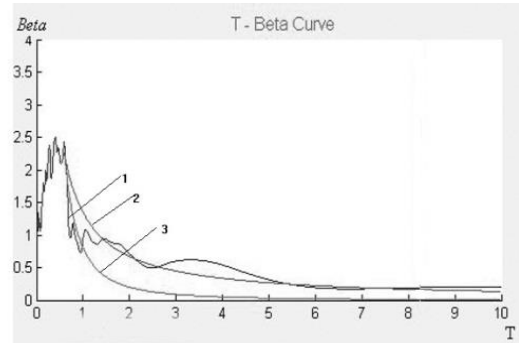
65. T2- 3-2 (1995 HYOUGOKEN-South,NS)



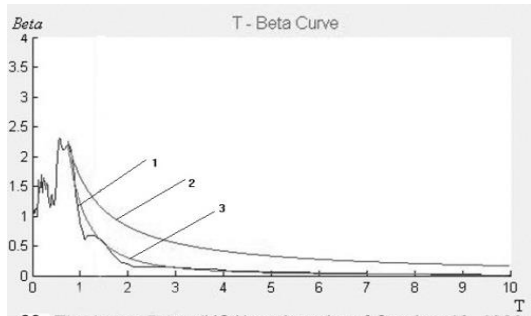
66. T2-3 - 3 (1995 HYOUGOKEN-South,EW)



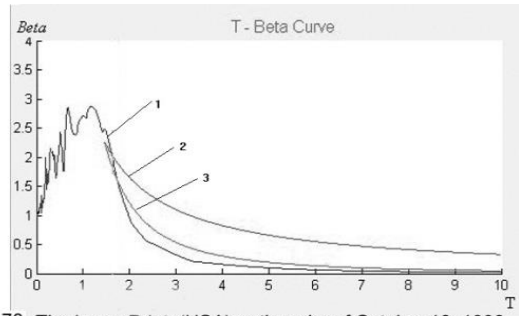
67. The Chichi(Taiwan)earthquake of September 21, 1999. Unknown recording Station. Longitudinal Component



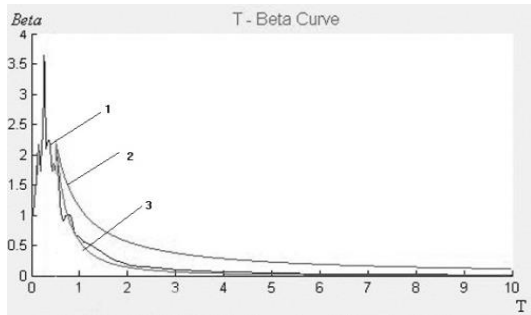
68. The Chichi (aiwan)earthquake of September 21, 1999. Unknown recording Station. Transversal Component



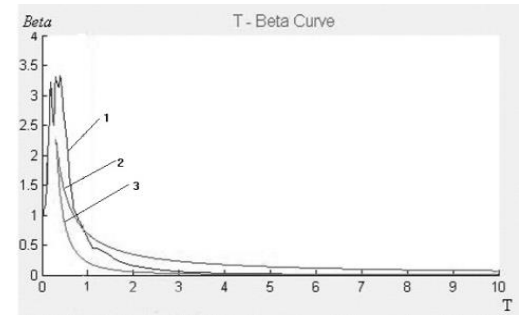
69. The Loma Prieta(USA)earthquake of October 18, 1989. Corralitos recording Station



70. The Loma Prieta(USA)earthquake of October 18, 1989. Emeryville recording Station



71. The Friulli(Italy)Earthquake of May 6, 1976. Unknown recording Station



72. The Hollister(USA)Earthquake of November 28, 1974. City Hall recording Station